

GOES-R series ABI Imagery artifacts

Mathew M. Gunshor,^{a,*} Timothy J. Schmit,^b David Pogorzala,^c
Scott Lindstrom,^a and James P. Nelson III^a

^aUniversity of Wisconsin–Madison, Cooperative Institute for Meteorological Satellite Studies,
Madison, Wisconsin, United States

^bNational Oceanographic and Atmospheric Administration, Center for Satellite Applications and
Research, Madison, Wisconsin, United States

^cCentauri, Chantilly, Virginia, United States

Abstract. The advanced baseline imager (ABI) on the Geostationary Operational Environmental Satellite (GOES)-R Series is a great improvement compared to the legacy GOES imager. For example, there are more spectral bands at improved spatial resolution and more frequent imagery. The vast majority of the images generated by the ABIs are free of visual defects, well calibrated, and produced in a timely fashion. Yet, there are rare times when visual artifacts, or anomalies, occur. Our study highlights and explains a number of these artifacts, some of which are traditional imagery defects for imagers such as striping and stray light, and colorfully named artifacts such as “caterpillar tracks” and “shark fins.” In addition, multiple resources are presented for more information about image quality and near-real-time image monitoring. © *The Authors. Published by SPIE under a Creative Commons Attribution 4.0 Unported License. Distribution or reproduction of this work in whole or in part requires full attribution of the original publication, including its DOI.* [DOI: [10.1117/1.JRS.14.032411](https://doi.org/10.1117/1.JRS.14.032411)]

Keywords: remote sensing; satellite; Geostationary Operational Environmental Satellite; advanced baseline imager; imagery; anomaly.

Paper 190899SS received Nov. 14, 2019; accepted for publication Aug. 4, 2020; published online Aug. 28, 2020; corrected Sep. 9, 2020.

1 Introduction

There are a wide variety of uses¹ of the imagery from the 16 spectral bands of the advanced baseline imager (ABI) on the Geostationary Operational Environmental Satellite (GOES)-R series. ABI has two spectral bands in the visible part of the electromagnetic spectrum, four in the near-infrared (NIR), and ten in the infrared (IR).² The spatial resolution of the bands varies between 0.5, 1, and 2 km at nadir. GOES-R, the first satellite in a series of four spacecraft that the United States will launch over the coming decade, became GOES-16 when it achieved geostationary orbit following launch on November 19, 2016. GOES-S, the second satellite in the series, was launched on March 1, 2018 and became GOES-17. GOES-16 became operational on December 18, 2017, in the GOES-East location (~75.2 deg W), and GOES-17 became operational on February 12, 2019, in the GOES-West location (~137.2 deg W). The GOES-R series is planned to be operational through the mid to late 2030s.

The vast majority of the images generated by the ABIs are free of visual defects, well calibrated^{3–7} and navigated,^{8,9} and produced in a timely fashion. Yet, there are rare times when visual artifacts, or anomalies, occur. Some of these anomalies are predictable based on satellite maintenance or time of year, but others may occur randomly. Many of these phenomena are so rare that most users, even ones who frequently analyze ABI imagery such as National Weather Service (NWS) field office forecasters, may not notice them. This paper highlights most of the known artifacts, and where possible, explains why they occur and when to expect them. In addition, several locations online will be noted where users can find out further information about GOES ABI related anomalies. In addition to educating users, such as operational forecasters, to the potential anomalies they may encounter in the imagery, another rationale to note these

*Address all correspondence to Mathew M. Gunshor, E-mail: matg@ssec.wisc.edu

artifacts, even if they occur infrequently, is the continuing use of GOES radiances for level 2 or derived products (such as cloud properties, fire characterization, atmospheric motions, volcanic ash detection, etc.) or in deep-learning algorithms.

2 Background

The ABI is typically operated in what is called mode 6, or “ten-minute full disk flex mode,”¹⁰ during which ABI acquires imagery covering three sectors at different temporal refresh rates. During a 10-min long mode 6 timeline, the ABI provides one full disk (or hemispheric) sector, two contiguous United States (CONUS) sectors, and twenty mesoscale sectors (usually split into meso1 and meso2 sectors, each of which can be covering a different region, nominally 1000 km × 1000 km at the subsatellite point, located anywhere on the full disk and scanned anew every minute). A timetable describing the mode 6 timeline appears in the GOES-R Product Definition and Users Guide (PUG).¹¹ It should be noted here that the CONUS sectors for the GOES-East and GOES-West satellites have different geographical coverage areas in that the GOES-East CONUS sector covers the 48 contiguous states and Puerto Rico, but the GOES-West version covers some of the western states, part of the eastern Pacific Ocean, includes Hawaii, and is referred to by many users as the Pacific United States, or “PACUS” sector. The 10-min repeat cycle means that not only earth scans are repeated at an even cadence—so too are calibration events, including space looks, views of the internal calibration target (ICT, i.e., blackbody for IR radiometric calibration, also called the IR calibration target), and star looks for use in image navigation. Note that the mode 6 timelines for GOES-16 and GOES-17 are slightly different (further discussed in Sec. 2.1).

GOES ABI data are provided to users as Network Common Data Form (NetCDF) files. Users can choose to obtain imagery either as calibrated radiances in the form of level-1b (L1b) or as level-2 cloud and moisture imagery product (CMIP) files. The CMIP files contain either reflectance factor for the visible and NIR bands or brightness temperature for the IR bands. CMIP files are produced as 16 single-band images for a given sector start time, with each channel maintaining its full spatial resolution. In addition there is also a multiband CMIP file available that includes all 16 bands at nominal 2 km resolution. With either L1b or L2 files, the only other pixel-level data provided are the data quality flags (DQF). DQFs can be used to determine if a pixel is good or usable. Metadata are also available in the files, in terms of variable attributes related to DQF, including percent of pixels considered good, percent of pixels considered out of range, etc. For full details, users are encouraged to consult the PUG.

There is more information on both GOES-16 and GOES-17 in terms of calibration accuracy and known issues in documents called “Maturity Release Readmes,” which are available on a National Oceanographic and Atmospheric Administration (NOAA) National Centers for Environmental Information (NCEI) website.¹² The “Readme” for the GOES-16 L1b radiances and CMIP files for full maturity is titled “GOES-16 ABI Level 1b and Cloud and Moisture Imagery (CMI) Release Full Validation Data Quality Product Performance Guide for Data Users,” dated September 24, 2019. Other L2 products (such as cloud properties, atmospheric motion vectors, sea and land surface temperature, atmospheric stability, and total precipitable water) are available as well, along with documents for GOES-17. Each GOES-R Series product has a separate algorithm theoretical basis document,¹³ and more information about the overall system is available from NOAA’s National Environmental Satellite, Data, and Information Service.¹⁴

A single ABI image is constructed from multiple swaths of the instrument detector arrays across the field of view, also referred to by some as the “field of regard,” which for the ABI typically means the same thing. A full disk image consists of 22 swaths, CONUS is comprised of 6 swaths, and each Mesoscale image is sampled with 2 swaths. Each swath is ~500 km north–south and consists of samples from hundreds of detectors in the north–south direction, the exact number being band-dependent, that are scanned from west to east. The timetables in the ABI PUG show how the swaths are interwoven between sector types.

The GOES-R website¹⁵ includes information about how ABI data are transmitted to users, and Ref. 16 contains more details on how the data are processed. Briefly, the process is as

follows. First, the ABI scans the Earth, part of space, and the ICT and transmits that raw data to the GOES-R ground system. The ground system then calibrates, navigates, and resamples the data to what is called the ABI Fixed Grid.¹⁷ The resultant pixels are then packaged and distributed as scaled radiances in NetCDF files that are transmitted via GOES ReBroadcast (GRB) to direct broadcast users. Select users who do not have a direct broadcast system can obtain data through an internet-based delivery system called product distribution and access (PDA). Furthermore, all users can access ABI data via NOAA's data archive system, the comprehensive large array-data stewardship system (CLASS) (which is populated via the PDA), several sites on the internet, or through a separate vendor. NOAA has also initiated the Big Data Project which provides data through various cloud providers (see Ref. 18 for details). NWS field offices receive a special, sectorized version of CMIP files through the Satellite Broadcast Network (SBN). Due to bandwidth issues, the sectorized CMIP full disk sectors are broadcast via the SBN at reduced spatial resolution.

2.1 GOES-17 ABI Loop Heat Pipe Anomaly

The GOES-17 ABI is operating in a degraded state due to an anomaly with its cooling system.¹⁹ The loop heat pipe (LHP) subsystem, which is designed to transfer heat from the ABI electronics and focal planes to the radiator, is not operating at its required capacity. There is more information online about this issue on the GOES-R series website.²⁰ For the purposes of this paper, the reader should know that this issue causes data anomalies unique to the GOES-17 ABI, and that part of the mitigation strategy includes operating GOES-17 using a slightly modified mode-6 timeline. Specifically, GOES-17 star looks are shortened and followed by nadir stares of the Earth, both of which help mitigate image and navigation artifacts due to the LHP anomaly. IR detectors on the GOES-17 ABI are all operating at a nominal temperature that is at least 20 K warmer than designed during the "stable" parts of the day, and at certain times of the year at temperatures over 40 K warmer during "hot" parts of the day. This has implications for how well the data can be calibrated, how well the band spectral response is known, the signal-to-noise ratio for each band, and other radiometric concerns. The detectors and electronics warm and cool on both diurnal and seasonal cycles. Near satellite noon when the Sun is behind the satellite, there is no direct path for photons to enter the aperture, and the LHP subsystem is able to maintain a stable temperature. During satellite night, when the Sun is on the opposite side of the Earth from the satellite, photons are able to enter the aperture and warm the focal plane modules (FPMs). The FPM temperatures do not peak exactly at satellite midnight, when the ABI is under maximum solar load, as one might expect. Instead, the maximum temperatures are observed a few hours later. This occurs because the cooling system is able to dissipate the extra heat for the hours leading up to satellite midnight, and for a short period afterward. After midnight when the cooling system is overwhelmed, the FPMs get too warm, and imagery for most of the IR bands is degraded. This diurnal nighttime warming is weakest near the summer and winter solstices and is strongest near (before and after) the two equinoxes. The unstable period of the day is especially problematic for calibration, since the rate of change of the warming is rapid enough to cause the nominal calibration schedules to be ineffective. For this reason, mode 6 on GOES-17 is different from that on GOES-16. The visible and near-IR (VNIR) band detectors are also operating at a higher temperature than desired, but they experience smaller diurnal variations compared to the IR and also are not affected as noticeably as the IR bands. At the time of this writing, most users and operators will not visually notice any impacts to the VNIR products; therefore, for this paper, this topic is only discussed in terms of how the IR bands are affected. This topic will be discussed further in Sec. 3.11.

3 Image Degradation, Artifacts, and Anomalies

This section introduces and describes several types of image degradation and/or anomalies that users may encounter when working with ABI data. They are presented in order of how frequently/likely they are to be encountered by routine users, from most to least. The anomalies unique to GOES-17 are presented last.

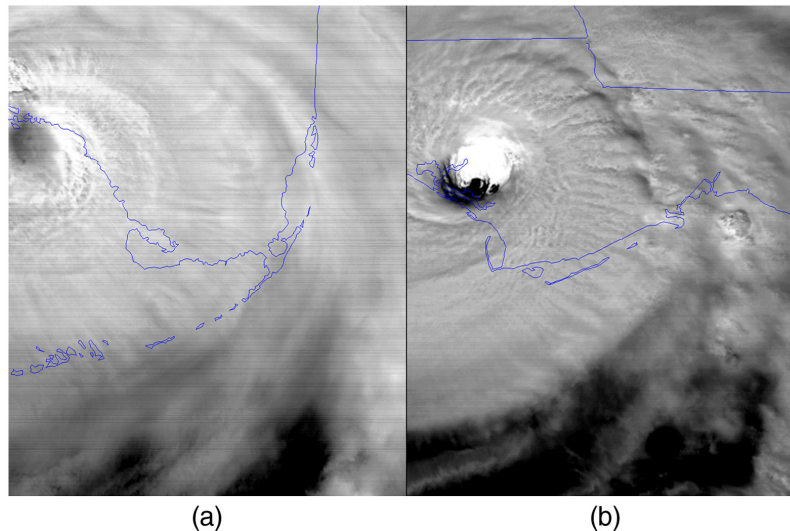


Fig. 1 GOES-16 band 2 ($0.64 \mu\text{m}$) for (a) Hurricane Irma and (b) Hurricane Michael. These images are from September 10, 2017 (18:57 UTC) and October 10, 2018 (17:57 UTC), respectively. Subtle detector-to-detector response variation gives rise to visible striping, most evident in the earlier image. Note that a special enhancement was applied to highlight striping in these images.

3.1 Striping

One of the most prevalent, though faint, artifacts that users may notice is low-contrast, widespread striping. This striping is typically most noticeable over certain scene types such as bright cloud (Fig. 1) or dark oceans. The striping is caused by subtle differences in how each of the hundreds of detectors responds to incoming light. Even though each detector is individually calibrated and meets requirements, small residual differences can remain. Image striping can be made more obvious by application of an image enhancement curve. Updates to operational algorithms and lookup tables have reduced striping to the point where users may no longer see it. Further mitigation measures are planned.

3.2 Bad Detector Stripes

Each ABI instrument downlinks radiant information from over 7000 detectors across the 16 bands. From time to time, one of these detectors may experience a sudden change in behavior, leading to a single, high-contrast stripe that appears once per swath. Unlike the more subtle striping discussed above, these stripes are visible regardless of the underlying scene content, as seen in Fig. 2. Depending on the exact nature of the problem, the mitigation steps vary. In some instances, a detector may “level-shift,” in which case its response to nominal earth radiance jumps higher or lower than previously. This anomaly can usually be addressed by product operators using routine data management scripts within a few hours. However, if the detector becomes saturated or unresponsive, the only fix is to command the instrument to begin using one of the redundant backup detectors in that row. These changes require engineering reviews and take several days to complete.

3.3 Incomplete Images

Incomplete images, an anomaly referred to by some as “dropped blocks” or “missing chunks,” are products that are missing a portion of the image data. The most likely causes are data drops at the GRB receiving station or via the transmission process to or from the PDA. Less likely causes include data drops within the level-0 (L0) to L1b processing in the GOES-R ground system, or even a missed collection by the instrument itself. The terms “block” and “chunk” have very specific meanings in data processing steps prior to the dissemination of data to users¹⁶ and some

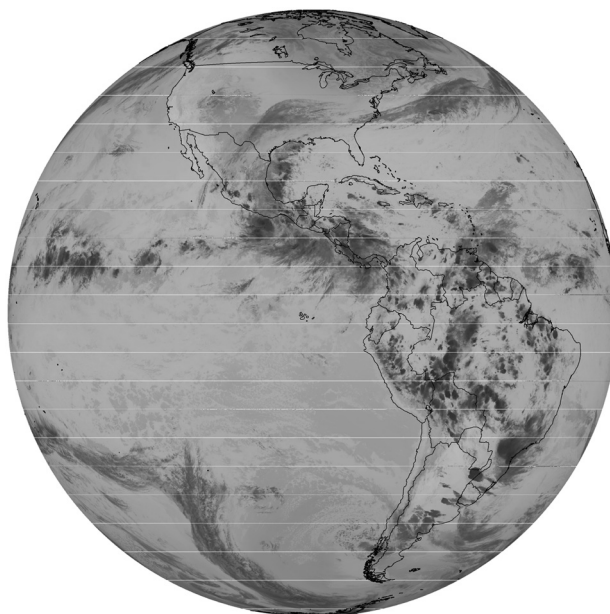


Fig. 2 GOES-17 band 11 ($8.4 \mu\text{m}$) full disk image acquired at 02:23 UTC on October 17, 2018. Detector #203 became saturated, resulting in high-contrast stripes in each swath until a backup detector could be used. The enhancement applied to this image has cold radiances mapped to darker colors, while the lighter grays are hotter radiances.

users adopted the terms “dropped blocks” and “missing chunks” to describe the phenomenon of missing data, though it would be difficult for a user typically to know what the cause of missing data is in any given case. If browsing for ABI imagery online, sometimes depending on the source’s method of ABI data acquisition, a user may encounter incomplete images. The missing data are typically contained within one swath (but can be larger), are not as wide as the entire swath, and often will be dropped from all 16 bands. Figure 3 shows an example of dropped blocks in GOES-16 ABI imagery where it appears an entire swath was dropped, plus part of the next, in the northern part of the full disk.

3.4 Bright Object Avoidance, AKA “Cookie Monster”

For the health and safety of the ABI, precautions were put in place to prevent it from directly viewing the Sun. This has most commonly been called Bright Object Avoidance, but the effect it has on full disk imagery has been nicknamed the “Cookie Monster effect,” since it appears as if someone has taken a bite out of the image (Fig. 4). From the ABI’s point of view, when the Sun is partially behind the Earth, the instrument will avoid scanning those parts of the swaths that are determined to be too close to the Sun’s direct rays.

The previous series of GOES largely avoided viewing direct sunlight during satellite eclipse seasons. All GOES have solar panels, which provide most of the onboard power for regular operation of the instruments. The GOES-I through M series did not have onboard batteries with enough capacity to operate all of the instruments when the satellite was in the Earth’s shadow. The GOES-NOP series had more capable batteries on board, allowing for some data collection at night during the satellite eclipse periods. The GOES-R series, however, is designed for 24 h, 365 days per year operation, and the so-called Cookie Monster effect is a result of the strategy employed to avoid damaging the detectors with direct sunlight.

The amount of data that is not scanned to avoid the Sun is band-dependent for a given scan time and is based on instrument design. The relative location of each band on the focal plane determines the size of the missing parts of the image. For example, in Fig. 5, note that the coverage of the states around the Gulf of Mexico is different for each band. This presents a unique challenge when combining bands since the edge of the missing area can vary. An example of combining three bands to generate an RGB image can be seen on the CIMSS Satellite Blog.²¹

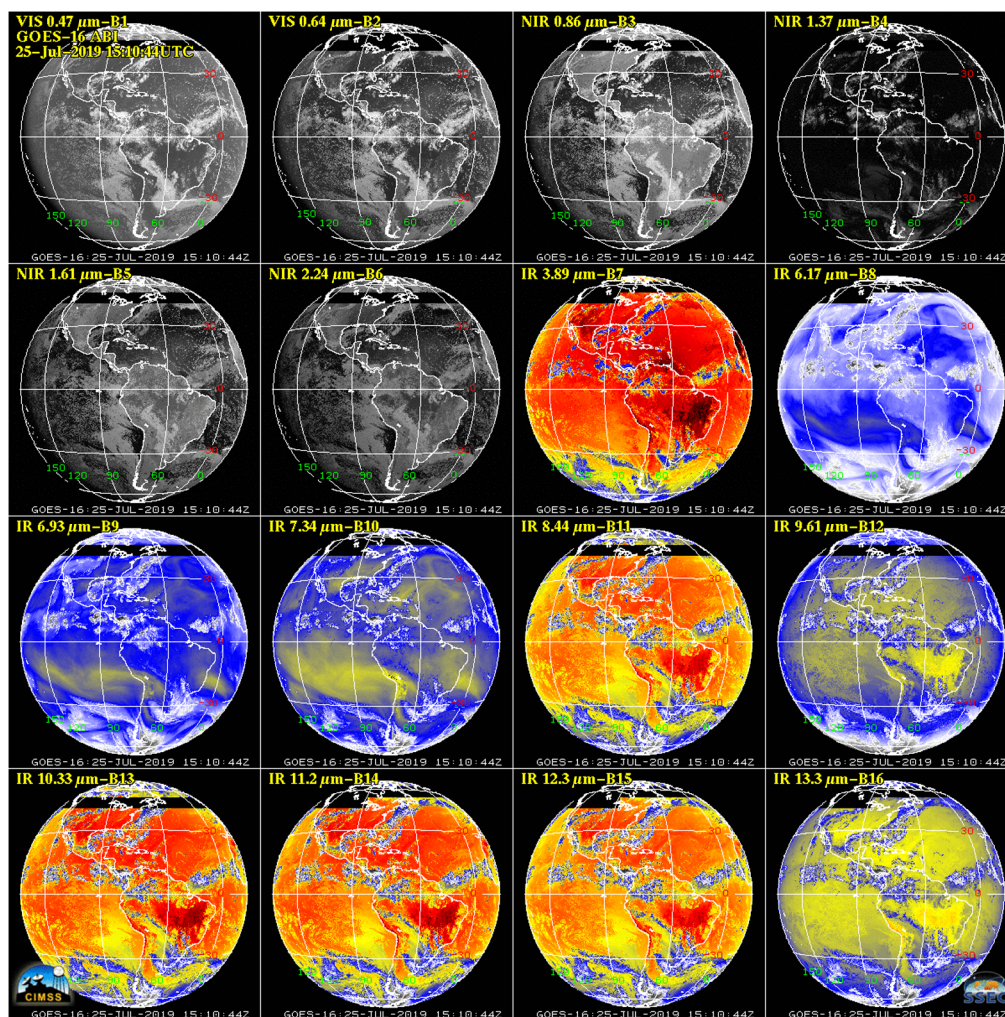


Fig. 3 Missing data appear (northern part of the images) as black in this 16-panel GOES-16 ABI image from July 25, 2019, at 15:10:44 UTC. For the 10 IR bands, red colors represent warmer brightness temperatures.

Users looking to combine bands in this manner are encouraged to utilize the DQFs, where bright object avoidance regions are currently flagged as “missing.”

3.5 Stray Light

Stray light is a familiar problem for GOES users. The term stray light refers to times when the instrument optics can detect, or be affected by, reflected light or emitted energy that is not coming from the Earth. Although the design of the instrument and the coupling of the instrument to the spacecraft were intended to minimize the possibility and effects of stray light, the problem still occurs on geostationary imagers, typically around the time of the solar equinoxes. There is more information on stray light, specifically how it affects data quality, known times of impacts, and relaxed data quality requirements at those times, in the Full Maturity Release Readme, referred to in Sec. 2. It is typically a problem at night, when the Sun is on the opposite side of the Earth from GOES and there is sunlight directly hitting the Earth-facing side of the spacecraft. Stray light may be a reflection of this sunlight or it may be caused by some part of the spacecraft or instrument being heated by the Sun and radiating that heat into the optical path. Stray light is often detectable in the visible/NIR imagery around the same times Bright Object Avoidance is implemented. A less well-known impact of stray light can occur when light enters the calibration measurements, typically when the ABI is doing a space look. This biases the

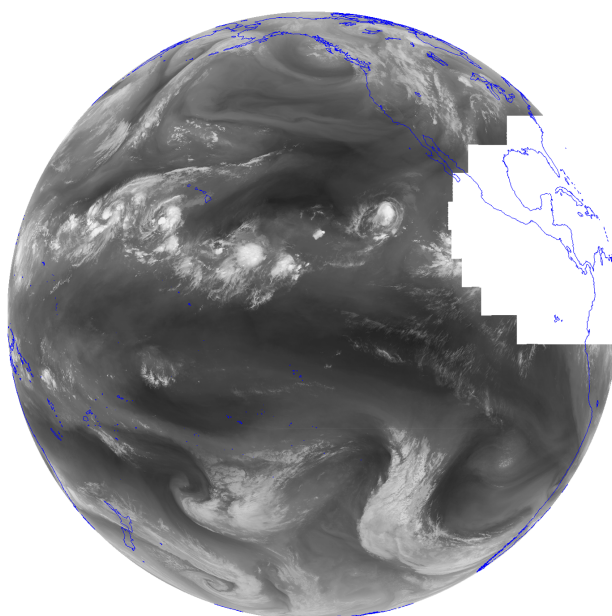


Fig. 4 Band 10 ($7.3 \mu\text{m}$) GOES-17 full disk ABI image from September 17, 2019, at 09:30 UTC showing the Solar Avoidance Zone, or “Cookie Monster.” This water vapor band has a grayscale enhancement applied, with colder temperatures appearing white and warmer temperatures appearing black.

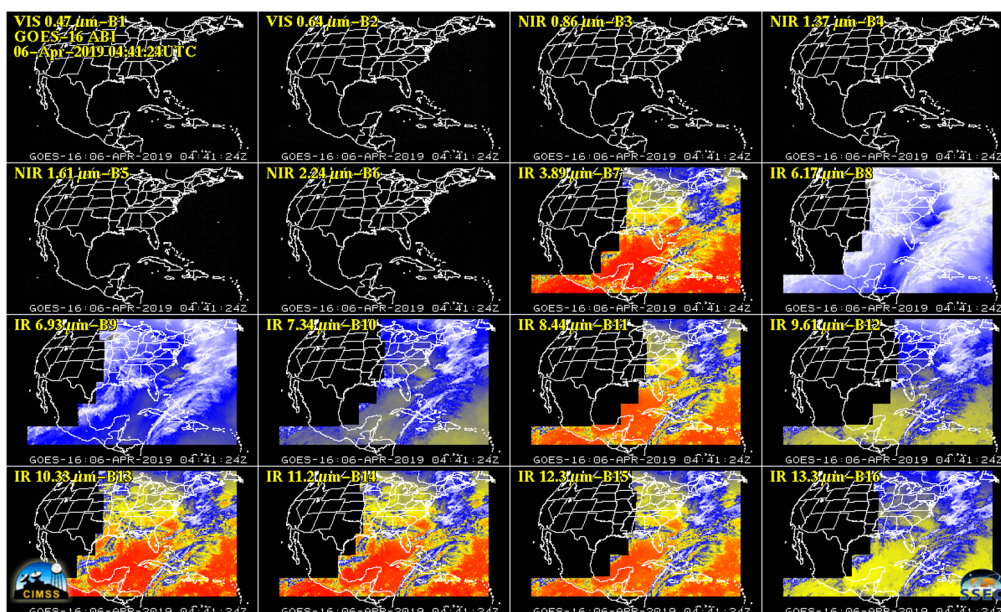


Fig. 5 The 16 bands of GOES-16 ABI on April 6, 2019, at 04:41:24 UTC, showing that the Solar Avoidance Zone has slightly different coverage for each spectral band.

space look measurement, negatively affecting the subsequent calibration of the images, or parts of images, that use that space look.

The most commonly seen stray light in ABI imagery manifests as “streaks” of bright pixels in the visible and NIR bands at night, which are otherwise dark (Fig. 6). Although users are not typically visualizing visible and NIR imagery at night, there is always a possibility that the stray light seen in those bands is also present in concurrent IR bands, but undetectable to the naked eye. The $3.9\text{-}\mu\text{m}$ short-wave IR band is particularly sensitive to reflected solar radiation

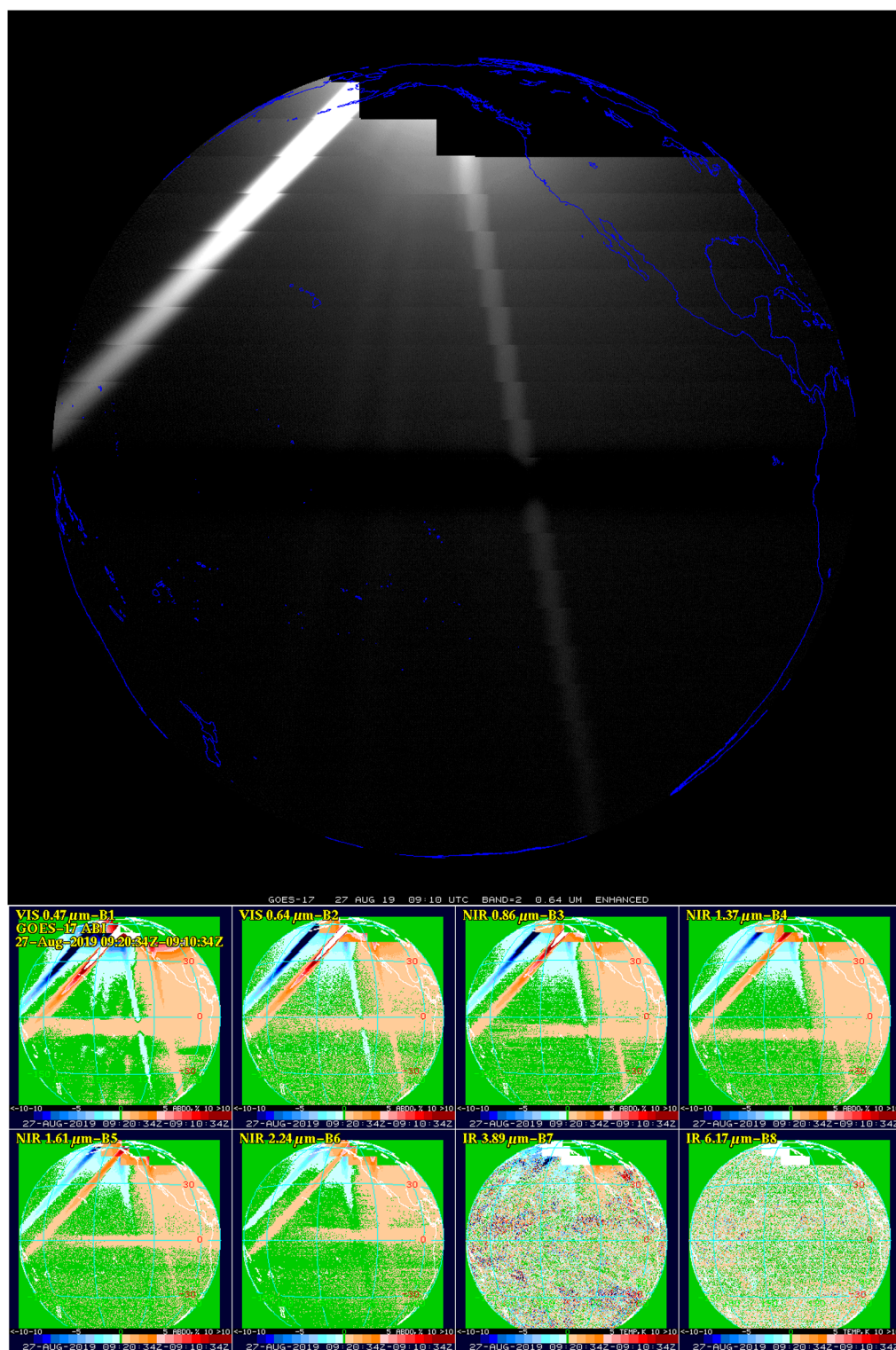


Fig. 6 Stray light seen in GOES-17 on August 27, 2019, at 09:10 UTC. The top panel shows band 2 ($0.64 \mu\text{m}$) with bright object avoidance at top of the image and various bright streaks through the image which, absent stray light, would be dark. The lower eight panels show bands 1 to 8 time-difference imagery where the 09:10 UTC image has been subtracted from the 09:20 UTC image. The effects of stray light on the imagery is apparent in this type of display, including in band 7 ($3.9 \mu\text{m}$), the shortwave window. The band across the equator, dark in the top image and seen in the difference images in the lower panels, is the result of when scattered light enters the space look region.

and can be affected by stray light at night. This can affect a band difference such as $3.9\ \mu\text{m}$ minus $10.3\ \mu\text{m}$ and may affect the quality of L2 products derived from this shortwave window band. As an example, the lower eight panels of Fig. 6 show time difference imagery where stray light shows up as positive (orange) and negative (blue) differences due to the angle of the Sun changing between 10-min full disk image times. The 7th of those 8 panels shows band 7, the $3.9\text{-}\mu\text{m}$ band. The large “streaks” of stray light in the VNIR bands, that seem to almost emanate from the missing area of the northern part of the full disk, are also evident in the time difference image of band 7. According to the GOES-16 Full Maturity Readme, stray light is allowed for ABI within 5 deg from the Sun (“restricted zone”) for the $3.9\text{-}\mu\text{m}$ channel (band 7), and within 3 deg for other IR channels. “Stray light in the restricted zone is often excessive for the $3.9\text{-}\mu\text{m}$ channel (band 7), small for the $6.2\text{-}\mu\text{m}$ channel (band 8), and negligible for other channels.” Within 7.5 deg from the Sun is the zone of reduced data quality (ZRDQ), where requirements for radiometric accuracy are relaxed by a factor of two. Typically, stray light in ZRDQ is smaller than required for the $3.9\text{-}\mu\text{m}$ channel (band 7) and negligible for other channels.

3.6 Cold Pixels Around Fires

All ABI products are spatially interpolated (resampled) to the fixed grid, a static coordinate system centered on the satellite subpoint. After calibrating each detector sample from counts to radiance, the ground processing algorithms locate each sample on the fixed grid and resample the radiances into the output pixels. The interpolation is weighted by a two-dimensional, Sinc-like kernel.¹⁶ The resulting radiances for any given pixel, therefore, include contributions from samples that have been given a negative weight. In nearly every case, this negative weighting is desired and has no detrimental effect on the L1b product. However, this can be an issue in band 7, the $3.9\text{-}\mu\text{m}$ short-wave IR band. This band has the highest dynamic range, utilizes the full 14 bits of information, and is adept at sensing fires and other hot spots. When these extremely large radiances receive a negative weight, the result can be an artificially low radiance in neighboring pixels. Careful observers have noticed these CPAF, the so-called CPAF effect. The cold pixels in band 7 can be cold enough to cause an observer to misinterpret them as clouds.

For this reason, a modified kernel for band 7 was implemented (on April 23, 2019, for GOES-16 and on April 18, 2019, for GOES-17) in the GOES-R ground system that reduces the negative tail in the truncated Sinc function. Figure 7 is from a May 1, 2019 CIMSS Satellite Blog post²² and shows an image from GOES-17 at 23:30 UTC on 17th February. The “old” truncated Sinc function (denoted “Original”) has generated a falsely cold pixel, appearing as white in this image, immediately southeast of the warmer (center) pixels shown in black. The cold pixel is not present when the new, improved kernel is used. Note, however, that even though the hottest pixel shown in the image has cooled by 2 K with the improved kernel, a fire is still obvious. Note that the modified kernel also results in slightly degraded

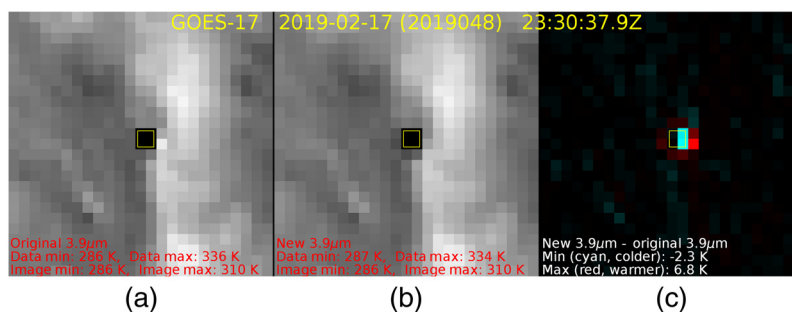


Fig. 7 GOES-17 $3.9\text{-}\mu\text{m}$ imagery in the vicinity of a fire at 23:30 UTC on February 17, 2019, with the former (a) interpolation scheme, (b) the updated interpolation scheme, and (c) the difference field between the two. The yellow outline (inside the black box in the leftmost two panels) shows the approximate fire location over Mexico. (Image courtesy Chris Schmidt, CIMSS)

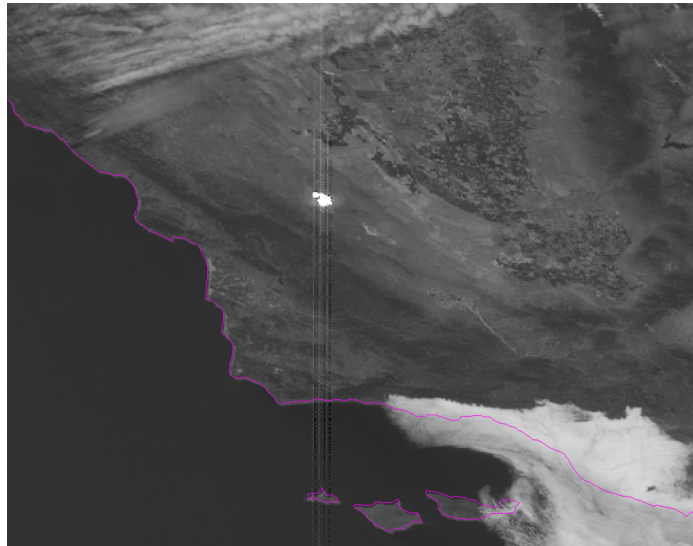


Fig. 8 A portion of the GOES-17 ABI band 2 ($0.64 \mu\text{m}$) CONUS image on June 07, 2019, at 18:31:19 UTC. The Topaz Solar Farm in southern California is clearly evident near the center of the image. The reflection from the solar panels also affected nearly all the detectors north and south.

spatial performance. This kernel should be implemented for GOES-T and GOES-U prelaunch, so the CPAF effect should not be seen for those satellites.

3.7 Solar Farms and Ringing

Several surface features, typically manmade, can produce interesting effects in ABI imagery. The most frequent is caused by solar farms—regions that can span hundreds of acres covered in solar panels designed to generate electricity. When the geometry between the Sun, these panels and an ABI is just right, the panels reflect sunlight directly into the ABI’s line-of-sight. The affected pixels appear warmer in the IR bands. In the visible and NIR bands the farms cause saturation and, in some cases, vertical striping. Users can expect to see this phenomenon in the western United States (Nevada, Colorado, California, and Arizona), which is home to the largest farms. If the panels are installed at fixed angles, this degradation will occur at a fixed solar incidence angle, meaning that it will occur numerous times throughout the year (unique to each farm’s location and the angle of their panels). Reflections off the roofs of large greenhouses have also been detected in the ABI visible bands.

Figure 8 shows the Topaz Solar Farm in southern California, a 19-km^2 farm located near $35:20 \text{ N}$, $120:04 \text{ W}$, at 18:31 UTC on June 7, 2019. The vertical stripes were noticeable every day around this time ($\sim 10:30 \text{ a.m.}$ local time) from May 30 through June 10, 2019. The solar farm itself is noticeable on many other days. For this case, the effects of solar farm glint appeared in all of the ABI bands except the water vapor bands (8 to 10), which typically do not detect surface features. This case even caused CPAF in band 7, despite the updated resampler kernel, and a similar effect was seen in band 2 ($0.64 \mu\text{m}$), with dark pixels neighboring the extremely bright ones (“ringing”).

3.8 RFI

Solar radio frequency interference (RFI) is a known phenomenon that also affected the previous GOES series. Solar RFI affects the ground station’s receiving antennas, adding noise to the signal that affects the quality of the subsequent images, mostly through missing data. Since solar RFI is caused by the Sun, it will affect a specific antenna at the same time of day on the same days of the year, which are fortunately infrequent. One possible solution would be to “share” data between multiple sites since ground stations that are far enough apart will experience RFI at different times.

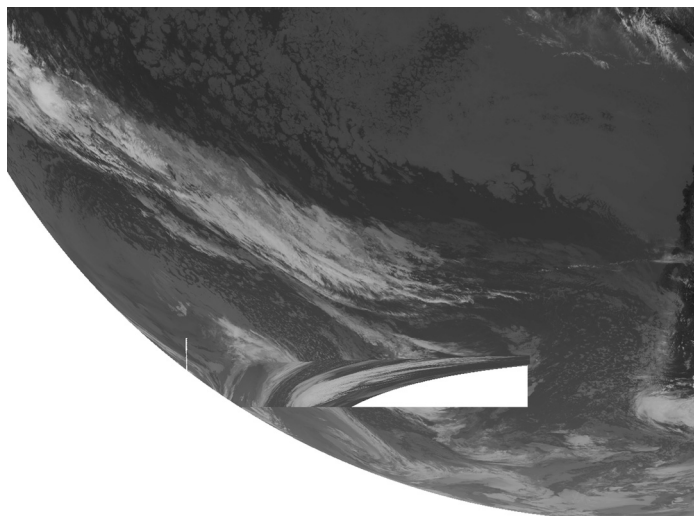


Fig. 9 GOES-16 ABI band 13 ($10.35\ \mu\text{m}$) on December 11, 2019, at 12:50 UTC, the southwest portion of a full disk, an example of both the “caterpillar track” and “shark fin” anomalies. Caterpillar tracks are somewhat small and easy to miss.

3.9 Caterpillar Tracks and Shark Fins

“Caterpillar tracks” and “shark fins” are so named for the way these anomalies manifest in imagery (Fig. 9). The narrow, vertical bands of missing data reminded some analysts of what it looks like when a caterpillar eats a track through vegetation. The shark fins are roughly triangular in shape, with missing data on one side and distorted data on the other. Both of these anomalies are short in duration and typically contained to a single swath. Shark fins almost always appear with caterpillar tracks nearby, but sometimes caterpillar tracks appear alone. The root cause is data packet loss at the level-0 stage, before the ground system resamples the raw detector data into the ABI fixed grid. The result for a caterpillar track is a section of missing data that is several pixels wide and spans the height of an entire swath. Given the unpredictable manner, in which the detector samples are located on the resampler kernel, the edges of the tracks appear jagged. Additionally, due to the nature of the level 0 data downlink and resampling algorithm, sometimes the caterpillar track may not be contiguous, with only occasional pixels missing along the column. The result for a shark fin is a nearly triangular shaped section of missing data with adjacent data from the same swath appearing to be distorted. Note that although there is a gap of missing data in a shark fin, the DQFs for these pixels are not marked as such. This is because during processing, the gap does not yet exist when DQF values are determined. Valid radiances exist, but they are being resampled into incorrect locations, resulting in a gap in the imagery.

At the time of this writing, this is an unpredictable anomaly that normally only impacts a few bands at a time and in somewhat different locations. The source of the problem and steps to mitigate it are both under investigation. For caterpillar tracks, it is thought that the relative E/W offsets of the track locations between different bands are dependent upon where an individual band’s detectors lie on the focal plane. Since the ABI normally scans from west to east, one can think of the bands being arrayed on the FPM west to east (though not ordered by wavelength). Similar to how the “cookie monster” effect varies per channel in the east–west direction, this too is displaced on the Earth since the different channels are viewing different locations at the time of packet loss.

3.10 HBT Thruster Flush

The propulsion system on each of the GOES-R series satellites uses two hypergolic hydrazine bipropellant thrusters (HBTs), which are used for relocation and decommissioning.³ As part of the normal operations of the satellite, these thrusters are flushed approximately every 240 days

throughout operations. This may cause a product outage lasting ~ 10 min and degraded product navigation for up to 45 min after the HBT flush. The extended navigation degradation is due to the fact that the ABI cannot scan during the flush (including for navigation), which causes the image navigation and registration (INR) processing¹⁷ to degrade. As examples of the HBT thruster flush, ~ 30 min of data were degraded on GOES-17 on July 10, 2019. On March 12, 2019, the GOES-16 HBT flush caused a reset of the Kalman filter used in ABI INR processing, resulting in almost 3 h of degraded image navigation. The GOES-16 HBT flush on October 30, 2019, had an outage of 10 min, followed by degraded data for ~ 10 min, which included degraded image navigation and some blank images. A mitigation to reduce this time of degraded imagery was worked into the system and first took effect for the GOES-17 HBT flush of March 10, 2020.

3.11 Loop Heat Pipe (GOES-17 Only)

An unfortunate mishap with the GOES-17 ABI LHP means that the instrument is unable to maintain the desired thermal state (see Sec. 2.1). At the worst (hottest) times of the day on the

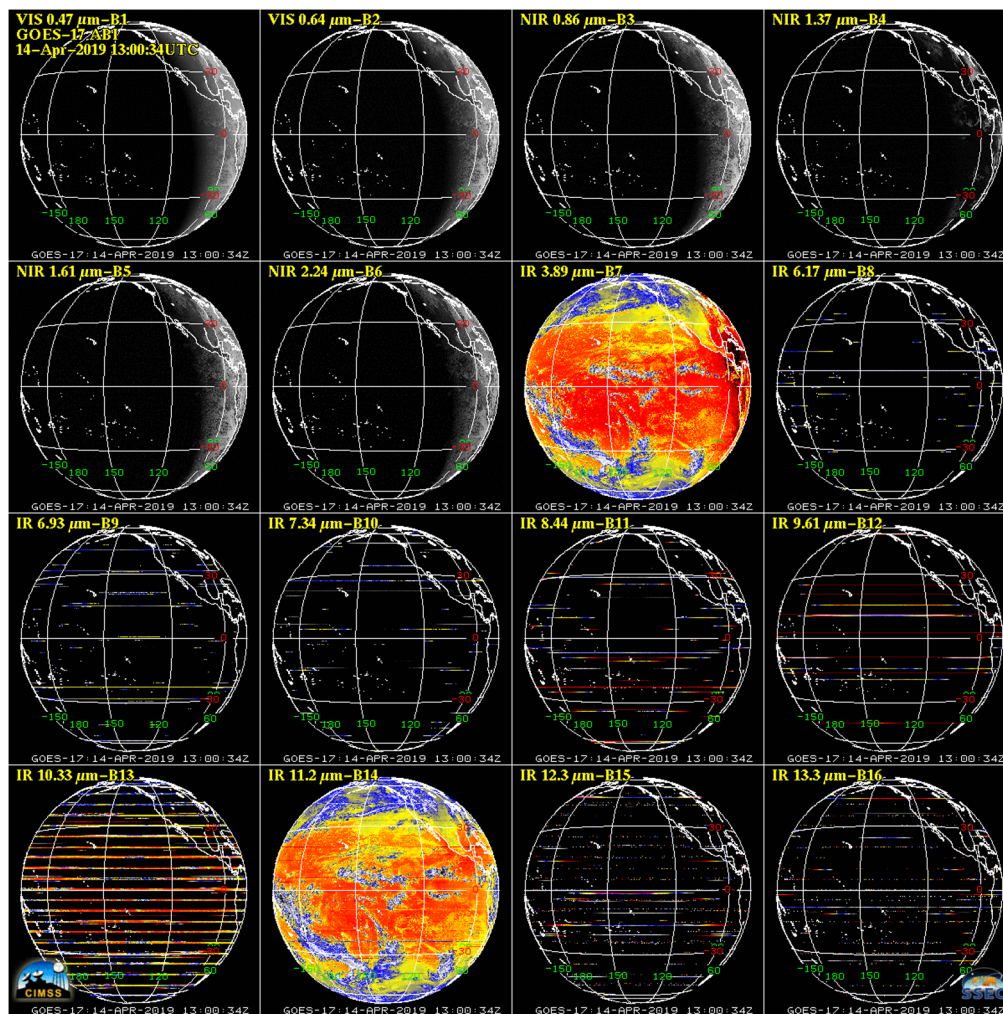


Fig. 10 All 16 bands of the GOES-17 ABI full disk on April 14, 2019, at 13:00:34 UTC. This is expected to be the hottest LHP day of the year for GOES-17, shortly after the spring equinox and right after GOES-17 exits spring eclipse. Bands 1 to 6 are not noticeably affected (visible/NIR bands at night are dark), short-wave IR band 7 is unaffected, IR window band 14 is somewhat affected (note some striping in addition to a bias that is not detectable by the naked eye), and the other IR bands are totally unusable.

worst days of the year (i.e., immediately before and after the equinoxes), all of the IR bands except band 7 are affected. Many of the bands become unusable for several hours each day, on days leading up to and following the equinoxes. Figure 10 shows the impact of the LHP anomaly in the worst-case scenario, the hottest day of the year for the instrument, April 14, 2019, as the satellite is just coming out of its eclipse period following the spring (vernal) equinox (March 20, 2019).

One of the issues for users is that during the unstable periods the data may look reasonable, but since the nominal calibration algorithm assumes cold, stable focal planes, it is unable to meet the expected radiometric accuracy and precision. To mitigate this, the instrument vendor developed an alternate calibration scheme known as predictive calibration (pCal). pCal went into operation on July 25, 2019. Results indicate that it is capable of improving data that were biased by several K, greatly improving radiometric accuracy, as well as the usability of the data.

Figure 11 highlights the dramatic improvement over the course of a day due to pCal, in this case showing band 10 ($7.3 \mu\text{m}$). This GEO-GEO comparison between GOES-16 and GOES-17 shows the difference (GOES-17 minus GOES-16) between the mean brightness temperatures in a 401×1001 pixel sized area centered on the equator at 106 deg west longitude. In this comparison, the data from each satellite have been remapped to a common projection to reduce the impact of view angle differences on the calculations. While this analysis does not fully characterize the calibration of each instrument, it is used to demonstrate both the impact of the LHP anomaly as well as the effectiveness of pCal. Test datasets were generated with the pCal algorithm turned off on October 12, 2019. This provided an opportunity to see a comparison of the data with and without pCal.

In the data without pCal implemented, the brightness temperature difference is stable and without much bias until just before 10:00 UTC. At this time, the LHP is no longer able to maintain the focal planes at a steady temperature. The images without pCal implemented between 10:00 and 18:00 UTC still look reasonable to the eye without many obvious defects such as striping or noise. The issue is that they are no longer well calibrated, demonstrating the problem for users in that images may appear to be reasonable, but during unstable times the original

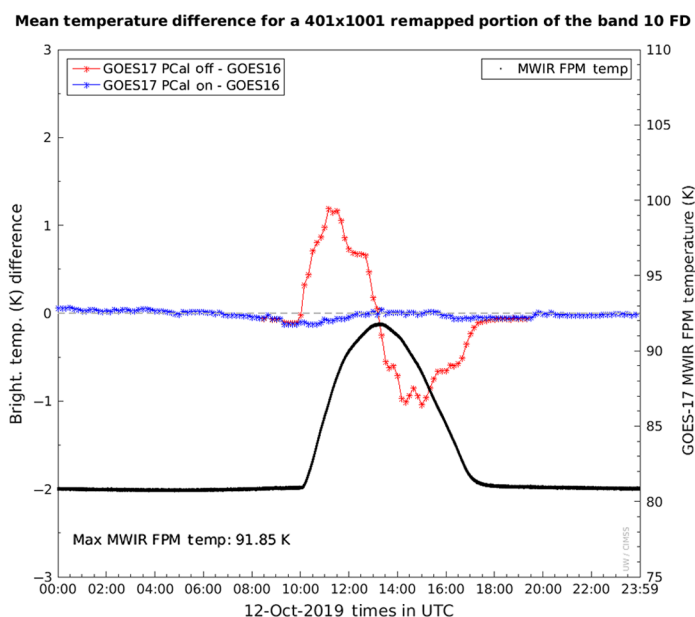


Fig. 11 The band 10 ($7.3 \mu\text{m}$) mean brightness temperature differences (GOES-17 minus GOES-16) on October 12, 2019 for a 401×1001 pixel sized box within the overlapping portions of the full disks centered halfway between the two satellites (on the equator and at 106 deg west longitude). The black line, whose values are shown on the right-hand y axis, is the MWIR FPM temperature in K. The red line shows the differences on a test system, with the pCal algorithm turned off, while the blue line shows the differences on the operational system, with pCal implemented normally.

calibration algorithm fails to provide the expected calibration accuracy because the internal temperatures are changing so rapidly. Without pCal, the radiometric bias during this time can be more than an order of magnitude greater than the specified noise for IR bands. The data with pCal implemented in Fig. 11 show how dramatic the pCal improvement was for this band and most of the other IR bands (not shown) on this day. For this day, this figure shows a much steadier and relatively small bias during the hottest time of the day for the FPM. pCal is not able to alleviate the issues seen at the hottest times of the year, such as in Fig. 10, when the detectors are saturated and cannot produce usable imagery. However, at times when data would have been impacted in terms of having a temperature bias, pCal adds hours of improved data quality on most days with elevated FPM temperatures.

Users looking at archived GOES-17 ABI data from before July 26, 2019, should be aware of the potential impacts of the heating issues on data as well as changes that were made to the L1b DQFs. The original DQFs for ABI L1b had possible integer values of 0 to 3. Good pixels are flagged 0, conditionally usable pixels are flagged 1, out of range pixels (sometimes referred to as saturated) are flagged as 2, and no value (sometimes referred to as missing) pixels are flagged as 3. Starting on April 8, 2019, an additional DQF value of 4 went into effect which signifies “above the FPM temperature threshold.” Some users have referred to this as the “temperature data quality flag” (TDQF), though it is not a separate quality flag variable from what previously existed for ABI. The FPM temperature is a relatively quick, but not perfect, indicator to predict when data are going to be unusable.

Included with the new per-pixel DQFs are new variables and attributes in the NetCDF files. Among these are the maximum FPM temperature during the scene collection time and the DQF = 4 temperature thresholds (increasing and decreasing). Upon initial implementation, these thresholds were set at 81.1 K for the long-wave IR bands (12 to 16) and 81.3 K for the mid-wave IR (MWIR) bands (8 to 11). These thresholds corresponded to the FPM temperatures during the cold, stable times of the day, and were meant to warn users when calibration might be impacted by warming detectors. Upon further analysis, these thresholds were deemed overzealous, flagging data that was otherwise well-calibrated and usable. On August 8, 2019, new thresholds were implemented that take into account the improved calibration from pCal. These thresholds are band-dependent and are no longer the same for both rising and falling FPM temperatures. The thresholds were refined once again on October 2, 2019. The DQF variable also includes an attribute called `percent_focal_plane_temperature_threshold_exceeded_qf`, which is another way for users to know how much of the image was scanned when the FPM was above the recommended usable temperature.

In February 2020, a modified scanning schedule was introduced for GOES-17 to mitigate the effects of the LHP issue. This was called the “GOES-17 ABI mode 3 cooling timeline” and was operated from 06:00 to 12:00 UTC (centered roughly on satellite midnight) from February 26, 2020, to March 01, 2020. The timeline will operate in mode 3 (“Flex mode 3” uploaded as `timelineID = 3`) where GOES-17 ABI will generate a single full disk once per 15 min and generate each mesoscale domain sector every other minute. This special cooling timeline has mode 3 in the name, but it is not the same as the original mode 3 timeline as in addition to the mesoscale sectors being scanned less often, the CONUS domain will not be scanned during the timeline as those periods will be used for cooling. Analysis of this timeline revealed that FPM temperatures were reduced by over 2 K and hence there was less time, in which some bands were totally unusable during those days. The mode was used again between 06:00 to 12:00 UTC from April 09 to May 01, 2020. Analysis conducted by the GOES-R Calibration Working Group (CWG) after May 1 showed that the daily peak FPM temperature was reduced by ~4 K, there was little to no impact for bands 7, 13, and 14, and it shortened the period of lost imagery by 30 to 90 min (channel dependent) for the other bands. For most bands and on most days, that meant 50 to 150 mesoscale images, 2 to 8 CONUS images, and 2 to 6 full disk images were available that would not otherwise have been usable. The biggest benefit was noticed on the cooling side of the daily heating period, which is after the instrument has returned from running the special timeline mode and hence CONUS images are available again. At the time of this writing, the plan is to operate this mode similarly from August 12 to September 01, 2020, and October 14 to October 31, 2020. Dates for 2021 will be determined later.

3.12 Lunar Intrusion into Spacelooks (GOES-17 Only)

One of the actions taken to mitigate the LHP anomaly was to disable the quality check of routine view of space (spacelooks). These spacelooks occur every 30 s during routine imaging, as well as immediately preceding each view of the ICT. If the illuminated moon happens to be in the view of the spacelook, the nominal calibration algorithms detect this, discard that spacelook, and reuse the previous one. However, for GOES-17, this “lunar intrusion threshold” is ineffective due to the increased operating temperature as a result of the LHP anomaly, so this rejection test is disabled. The result is that spacelooks that do include the moon can lead to two types of calibration artifacts.

The first type of lunar intrusion artifact occurs when the moon is in the view of one of the routine spacelooks. The result is that the difference between the signal from the Earth and space (“delta counts”) is smaller than it should be. In this situation, the ensuing swath appears darker than its neighbors, as seen near the bottom edge of the image in Fig. 12. This artifact only persists for a single swath, since the next swath will acquire its spacelook in a different location.

The second type of lunar intrusion, shown in Fig. 13, occurs when the moon appears in the spacelook preceding a view of the blackbody. While the routine spacelook intrusion can occur monthly (depending on the relative locations of the Sun, Earth, Moon, and Satellite), this second type is much less frequent (1 to 2 times per year). However, the impact is much more noticeable. In this case, the corrupted spacelook impacts the calibration coefficients for most detectors in multiple spectral bands and persists until the next view of the ICT. Multiple options to mitigate this artifact are being discussed by the GOES-R Program, but as of the time of publication, none have been implemented operationally.

3.13 Yaw Flip (GOES-17 Only)

A yaw flip is a 180-deg rotation about the nadir axis of the satellite. Although sometimes used on the previous GOES series (e.g., GOES-15) to improve seasonal radiometric performance, the GOES-R series was designed to not require semiannual yaw flips during normal operations, only while in storage mode. Unfortunately, the GOES-17 LHP issue has made yaw flips necessary for GOES-17 to reduce the solar load on the instrument. On September 9, 2019, the outage due to a yaw flip maneuver lasted 30 min, with an additional 30 min for VNIR bands to stabilize and longer for the IR bands. It included both partially scanned and poorly navigated images. There is a plan to mitigate this so the system should recover faster from future yaw flips.

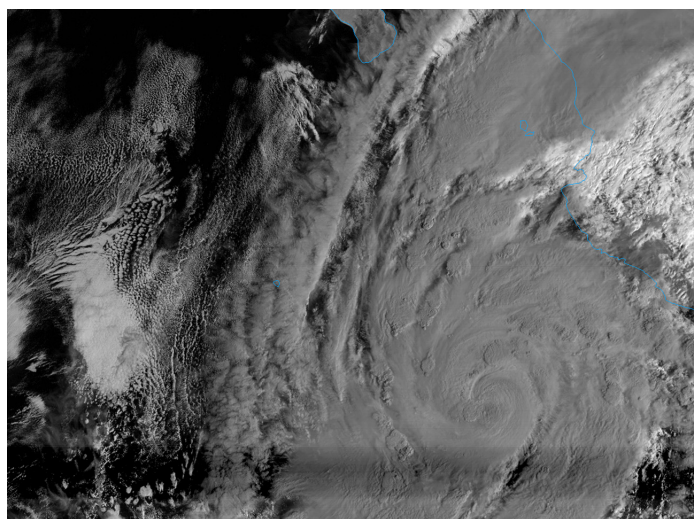


Fig. 12 GOES-17 band 5 ($1.61 \mu\text{m}$) enhanced subset of CONUS image off the west coast of Mexico from October 21, 2018 14:52 UTC, showing the effects of the moon intruding into the Spacelook taken prior to the image. The lunar intrusion leads to a darkened band, seen here at the bottom of the image.

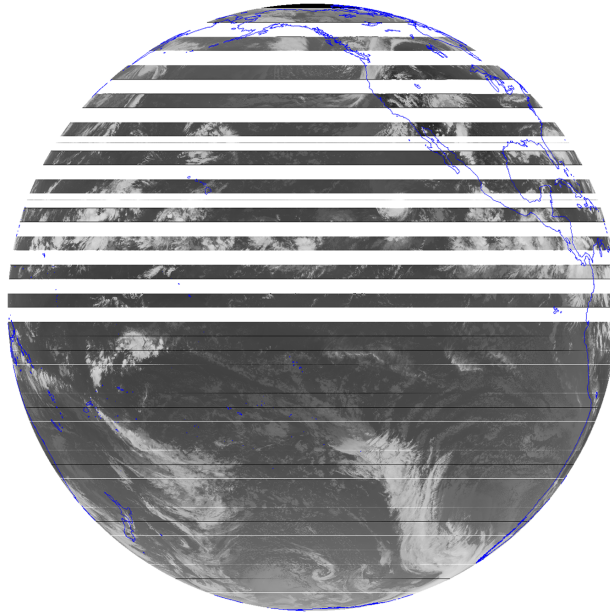


Fig. 13 GOES-17 full disk band 13 ($10.3 \mu\text{m}$) image on September 15, 2019, at 23:10 UTC, showing banding caused by lunar intrusion to the spacelook immediately preceding an ICT look.

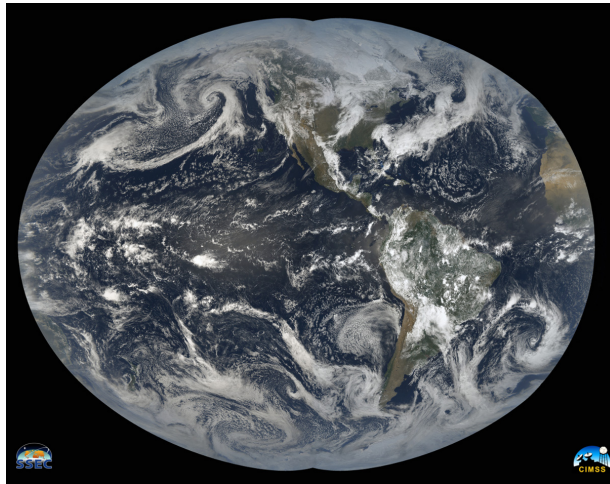


Fig. 14 Mollweide projection image combining CIMSS natural color GOES-17 (West) and GOES-16 (East) ABI imagery during the 2019 Spring Equinox (March 20, 2019). This image was produced by progressively combining 2.5° longitudinal sections of illumination at local solar noon—beginning at 12 UTC March 20 in the east and ending at 03 UTC March 21 in the west.

4 Conclusion

Overall, the vast majority of the imagery sensed by the ABI instruments on GOES-16 and -17 is well-calibrated, well-navigated, and free of obvious visual defects. The ABIs on GOES-R series satellites serve as tremendous tools for forecasters and others, providing spectacular imagery that covers much of the globe from western Africa in the east to New Zealand in the west (Fig. 14). On occasion, users may notice some of the image anomalies mentioned in this paper. If encountering a suspected anomaly, users can access multiple online resources to find out more information.

NOAA's Office of Satellite and Product Operations (OSPO), frequently referred to by users as NOAA Operations, maintains an e-mail list that users can subscribe to which NOAA Operations uses to warn of upcoming events. Events such as the GOES-17 semiannual yaw

flip, HBT Thruster Flush, Mesoscale sector locations, and other planned events are announced up to days in advance. Other data outages that may be caused by something unforeseen, such as a hardware failure or power outage, are often explained soon after they occur. General satellite messages from OSPO appear on the following web page.²³ To get all of the updates, users can subscribe to the ESPO Operations e-mail distribution list.²⁴ To report an issue, users are encouraged to e-mail user services.²⁵

The GOES-R CWG also maintains a web page to log significant calibration events for both GOES-16 and GOES-17. These will usually appear on their web page some days after the event, after they have had a chance to analyze it. That web page can be found in Ref. 26.

The CWG also maintains a website to monitor GOES calibration and navigation accuracy in real time, as well as provide plots of older data. This website provides monitoring of product quality, calibration measurements, and instrument status.²⁷

The NCEI at NOAA maintains a website on the GOES-R series that includes data access, information about products, and the Maturity Release Readme files each product team has written. At the time of this publication, the GOES-16 Radiances (and CMI) Full Maturity Readmes and the GOES-17 Provisional Maturity Readmes are available in Ref. 12. Furthermore, GOES-17 ABI passed full maturity status on February 19, 2020. More detailed information about radiometric accuracy, navigation and registration accuracy, and image quality can be found in these Readme documents, also referred to as GOES-16 or GOES-17 “ABI Level 1b and CMI Release Full Validation Data Quality Product Performance Guide for Data Users” documents.

Researchers at the University of Wisconsin–Madison also provide some monitoring tools for GOES-16 and GOES-17 online. One web site designed primarily to help monitor GOES-17 LHP issues by comparing GOES-17 to GOES-16 can be found in Refs. 28 and 29, providing 16-panel static and time-difference imagery. These URLs, along with most of the other URLs noted in this paper, can be found in Ref. 30. This page includes links to ABI imagery, calibration information, ABI timelines, scientific papers, and derived products.

Finally, the University of Wisconsin–Madison CIMSS Satellite Blog is an excellent resource for the explanation of anomalies as they occur. The primary goal of the blog is to highlight interesting meteorological phenomena and demonstrate satellite imagery as a tool for helping meteorologists. It is also used to help users understand imagery-related information. For example, the following blog entry details GOES-17 TDQF-related information³¹ and the blog can be searched based on categories, such as “calibration/anomalies.”

Acknowledgments

The views, opinions, and findings contained in this paper are those of the authors and should not be construed as an official National Oceanic and Atmospheric Administration or United States Government position, policy, or decision. The authors thank NOAA cooperative institutes, the Calibration, Product, and Algorithm Working Groups, the GOES-R Product Readiness and Operations team, and the GOES-R Program Office. Thanks to the many groups that made the ABI possible, including from the government, private industry, and academia. Special thanks to Chris Schmidt (UW-Madison Space Science and Engineering Center) for Fig. 7, Rick Kohrs (UW-Madison Space Science and Engineering Center) for Fig. 14, and the efforts of the GOES-R Algorithm Working Group Imagery team. The anonymous reviewers are also thanked for their detailed comments. ABI data are archived at NOAA’s CLASS.³² McIDAS-X was used for the generation of the majority of images in this paper. This research was supported in part by a NOAA grant to the Cooperative Institute for Meteorological Satellite Studies at the University of Wisconsin–Madison (NOAA, Award No. NA15NES4320001).

References

1. T. J. Schmit et al., “Applications of the 16 spectral bands on the advanced baseline imager (ABI),” *J. Oper. Meteor.* **6**(4), 33–46 (2018).
2. T. J. Schmit et al., “A closer look at the ABI on the GOES-R Series,” *Bull. Am. Meteor. Soc.* **98**(4), 681–698 (2017).

3. F. Yu et al., “Early radiometric calibration performances of GOES-16 advanced baseline imager,” *Proc. SPIE* **10402**, 104020S (2017).
4. J. P. Fulbright et al., “Calibration/validation status for GOES-16 L1b data products,” *Proc. SPIE* **10402**, 104020T (2017).
5. Z. Wang, “Radiometric quality assessment of GOES-16 ABI L1b images,” *Proc. SPIE* **10764**, 107641T (2018).
6. B. Bartlett et al., “Independent validation of the advanced baseline imager (ABI) on NOAA’s GOES-16: post-launch ABI airborne science field campaign results,” *Proc. SPIE* **10764**, 107640H (2018).
7. F. Yu et al., “Radiometric calibration performance of GOES-17 advanced baseline imager (ABI),” *Proc. SPIE* **11127**, 111271C (2019).
8. F. Yu et al., “Validation of early GOES-16 ABI on-orbit geometrical calibration accuracy using SNO method,” *Proc. SPIE* **10402**, 104020U (2017).
9. B. Tan et al., “GOES-16 and GOES-17 ABI INR assessment,” *Proc. SPIE* **11127**, 111271D (2019).
10. National Aeronautics and Space Administration (NASA) GOES-R Series Program Office, “GOES-R series data book,” Revision A, <https://www.goes-r.gov/downloads/resources/documents/GOES-RSeriesDataBook.pdf> (2019).
11. U.S. Department of Commerce (DOC), National Oceanic and Atmospheric Administration (NOAA), NOAA Satellite and Information Service (NESDIS), & National Aeronautics and Space Administration (NASA), “GOES-R Product Definition and Users’ Guide (PUG) Volume 3 (L1b Products),” Revision 2.2, <https://www.goes-r.gov/users/docs/PUG-L1b-vol3.pdf> (2019).
12. NOAA National Centers for Environmental Information (NCEI) formerly known as National Climatic Data Center (NCDC), “GOES-R series satellites,” <https://www.ncdc.noaa.gov/data-access/satellite-data/goes-r-series-satellites> (2020).
13. NOAA, National Environmental Satellite, Data, and Information Service (NESDIS), Center for Satellite Applications and Research (STAR), “GOES-R algorithm theoretical basis documents,” https://www.star.nesdis.noaa.gov/goesr/documentation_ATBDs.php (2019).
14. NOAA, National Environmental Satellite, Data, and Information Service (NESDIS), “GOES Overview,” https://www.noaasis.noaa.gov/GOES/goes_overview.html.
15. National Oceanic and Atmospheric Administration (NOAA) & National Aeronautics and Space Administration (NASA), “Geostationary operational environmental satellites—R series,” <https://www.goes-r.gov/>.
16. S. Kalluri et al., “From photons to pixels: processing data from the advanced baseline imager,” *Remote Sens.* **10**, 177 (2018).
17. B. P. Gibbs and J. L. Carr, “GOES-R orbit and instrument attitude determination,” in *24th Int. Symp. Space Flight Dyn.*, Maryland, pp. S8–3 (2014). http://issfd.org/ISSFD_2014/ISSFD24_Paper_S8-3_Gibbs.pdf.
18. NOAA, National Centers for Environmental Information (NCEI) formerly known as National Climatic Data Center (NCDC), “GOES-R series satellite data in the NOAA big data project,” <https://www.ncdc.noaa.gov/data-access/satellite-data/satellite-data-noaa-big-data-project> (2020).
19. J. McCorkel et al., “GOES-17 advanced baseline imager performance recovery summary,” in *Proc. IGARSS 2019—IEEE Int. Geosci. and Remote Sens. Symp.*, Yokohama (2019). <https://ntrs.nasa.gov/search.jsp?R=20190028689>.
20. National Oceanic and Atmospheric Administration (NOAA) & National Aeronautics and Space Administration (NASA), “GOES-17 ABI performance | GOES-R series,” <https://www.goes-r.gov/users/GOES-17-ABI-Performance.html>.
21. Lindstrom, Scott, “GOES-16 ABI RGB product artifacts related to keep out zones,” <https://cimss.ssec.wisc.edu/satellite-blog/archives/27662> (2018).
22. Lindstrom, Scott, “Change to the GOES-R ABI band 7 (3.9 μm) resampler,” <https://cimss.ssec.wisc.edu/satellite-blog/archives/33096> (2019).
23. NOAA National Environmental Satellite, Data, and Information Service (NESDIS), “General satellite messages—office of satellite and product operations,” <https://www.ospo.noaa.gov/Operations/messages.html>.

24. ESPCOperations@noaa.gov.
25. SPSD.Userservices@noaa.gov.
26. NOAA, NESDIS, STAR, "STAR-GOES-R calibration event log, https://www.star.nesdis.noaa.gov/GOESCal/goes_SatelliteAnomalies.php.
27. NOAA, NESDIS, STAR, "STAR GOES instruments calibration STAR GOES calibration validation-About GOES calibration <https://www.star.nesdis.noaa.gov/GOESCal/> (2020).
28. Cooperative institute for meteorological satellite studies (CIMSS) at the University of Wisconsin-Madison, "GOES-R series activities-CIMSS/SSEC, UW-Madison," http://cimss.ssec.wisc.edu/goes-r/abi-/16band_mainmenu.html (2020).
29. CIMSS, UW-Madison, "GOES statistics displays," http://cimss.ssec.wisc.edu/goes-r/abi-/static_and_timediff_imagery.html.
30. Schmit, Tim, "GOES-16 (and -17) images and information," <http://cimss.ssec.wisc.edu/goes/goesdata.html> (2020).
31. Schmit, Tim, "GOES-17 ABI temperature data quality flags (TDQF) thresholds updated," <https://cimss.ssec.wisc.edu/satellite-blog/archives/33832> (2019).
32. NOAA, "NOAA's comprehensive large array-data stewardship system," <https://www.class.noaa.gov/>.

Mathew M. Gunshor received his BSE degree in ocean engineering from Purdue University in 1993 and his MS degree in oceanography from Louisiana State University in 1997. He is a research scientist at the University of Wisconsin-Madison's Cooperative Institute for Meteorological Satellite Studies (CIMSS). His focus is on applied research projects in the areas of instrument design, algorithm development, data evaluation, training/user support, and identifying future needs. He has worked on ABI since 1999: band selection studies, algorithm development, waiver analyses, user training, postlaunch tests, and transition to operations.

Timothy J. Schmit received his bachelor's and master's degrees from the University of Wisconsin-Madison. He has dedicated his career to scientific support of multiple GOES missions. His research interests include calibration, visualization, and algorithm development and he is committed to research-to-operations, training others, and science communication. He has received the Department of Commerce Gold Medal, NWA Fujita Research Achievement Award, a finalist for the Samuel J. Heyman Service to America Award, and was recently elected a Fellow of the AMS.

David Pogorzala is a remote sensing scientist supporting the GOES-R Product Readiness and Operations Team. He joined GOES-R as a member of the Calibration Working Group in 2011 supporting analysis of prelaunch ABI data and modeling on-orbit performance. Since 2014, he has been the Cal/Val Tool Manager, overseeing development of science analysis tools. Prior to GOES-R, he was a staff scientist at the Digital Imaging and Remote Sensing Lab at the Rochester Institute of Technology.

Scott Lindstrom holds a BS degree in meteorology from Penn State University and MS and PhD degrees from the University of Wisconsin-Madison. Much of his recent work has focused on training USA National Weather Service forecasters on the use of GOES-R and JPSS Satellite Imagery and Products. For some of that work, he co-received the Larry R. Johnson Award from the National Weather Association in 2019. He writes a blog on fog (<https://fusedfog.ssec.wisc.edu>) and is a frequent author at the CIMSS Satellite blog (<https://cimss.ssec.wisc.edu/satellite-blog>).

James P. Nelson III received his BS and MS degrees in meteorology from the University of Wisconsin-Madison. He has spent the vast majority of his career working in the realm of computer software, focusing initially on software documentation, then branching out to develop meteorological product software, meteorologically focused visualization software, and writing supporting UNIX software. He has been intimately involved with the McIDAS-X software package for many years.